Relative importance of meridional and zonal sea surface temperature gradients for the onset of the ice ages and Pliocene-Pleistocene climate evolution

Christopher M. Brierley[1] and Alexey V. Fedorov[1]

Received 12 June 2009; revised 22 December 2009; accepted 13 January 2010; published 23 June 2010.

[1] During the early Pliocene (roughly 4 Myr ago), the ocean warm water pool extended over most of the tropics. Subsequently, the warm pool gradually contracted toward the equator, while midlatitudes and subpolar regions cooled, establishing a meridional sea surface temperature (SST) gradient comparable to the modern about 2 Myr ago (as estimated on the eastern side of the Pacific). The zonal SST gradient along the equator, virtually nonexistent in the early Pliocene, reached modern values between 1 and 2 Myr ago. Here, we use an atmospheric general circulation model to investigate the relative roles of the changes in the meridional and zonal temperature gradients for the onset of glacial cycles and for Pliocene-Pleistocene climate evolution in general. We show that the increase in the meridional SST gradient reduces air temperature and increases snowfall over most of North America, both factors favorable to ice sheet inception. The impacts of changes in the zonal gradient, while also important over North America, are somewhat weaker than those caused by meridional temperature variations. The establishment of the modern meridional and zonal SST distributions leads to roughly 3.2°C and 0.6°C decreases in global mean temperature, respectively. Changes in the two gradients also have large regional consequences, including aridification of Africa (both gradients) and strengthening of the Indian monsoon (zonal gradient). Ultimately, this study suggests that the growth of Northern Hemisphere ice sheets is a result of the global cooling of Earth's climate since 4 Myr rather than its initial cause. Thus, reproducing the correct changes in the SST distribution is critical for a model to simulate the transition from the warm early Pliocene to a colder Pleistocene climate.

Citation: Brierley, C. M., and A. V. Fedorov (2010), Relative importance of meridional and zonal sea surface temperature gradients for the onset of the ice ages and Pliocene-Pleistocene climate evolution, *Paleoceanography*, *25*, PA2214, doi:10.1029/2009PA001809.

1. Introduction

[2] Over the past 60–70 Myr, since the beginning of the Cenozoic when temperatures in polar regions were about 10°C, the Earth experienced an erratic cooling that culminated in the onset of glacial cycles in the Northern Hemisphere [*Zachos et al.*, 2001]. Even though the exact timing for this onset has not been firmly established, evidence suggests it had already begun by 2.7 Myr ago [*Haug et al.*, 1999; *Bartoli et al.*, 2005], leading to the recent reclassification of the start of the Pleistocene [*Gibbard et al.*, 2009]. The origin of Northern Hemisphere glaciation, and mechanisms of the gradual amplification of glacial cycles since the late Pliocene, remains a subject of persistent discussion (see, for example, the review of *Raymo and Huybers* [2008]). Other changes in Earth's climate during the past 5 Myr are also the subject of intense investigation, for example, the aridification of Africa since 3 Myr [*Marlow et al.*, 2000; *deMenocal*, 2004; *Dupont et al.*, 2005].

[3] Variations in solar radiation related to Milankovitch cycles (caused by periodic variations in orbital parameters such as the tilt of the Earth's axis) are responsible for the waxing and waning of the ice sheets [*Muller and MacDonald*, 2000]. However, the exact mechanisms by which these modest, perfectly periodic solar variations cause large variations in Earth's climate remain unclear. Apparently, Milankovitch forcing has been relatively constant over the past several million years [*Laskar et al.*, 2004], but the amplitude of the climatic response has been changing as long-term global cooling introduced different climate feedbacks (Figure 1).

[4] There are a number of different hypotheses for the Pliocene climate changes (many incorporating amplification by ice albedo feedbacks), but none has become the accepted reason for the onset of glaciation. *Lunt et al.* [2008] attempted to test a variety of these hypotheses using a coupled climate model and an ice sheet model. They found that a reduction in the atmospheric CO_2 concentration is essential for large-scale ice sheet growth on Greenland but not sufficient to explain the phenomenon. In fact, it appears that a stronger drop in CO_2 is required for the glaciation onset than is observed [*Pagani et al.*, 2010].

[5] Recently, changes in sea surface temperatures (SSTs) since the early Pliocene have attracted attention as a

[1]Department of Geology and Geophysics, Yale University, New Haven, Connecticut, USA.

0883-8305/10/2009PA001809

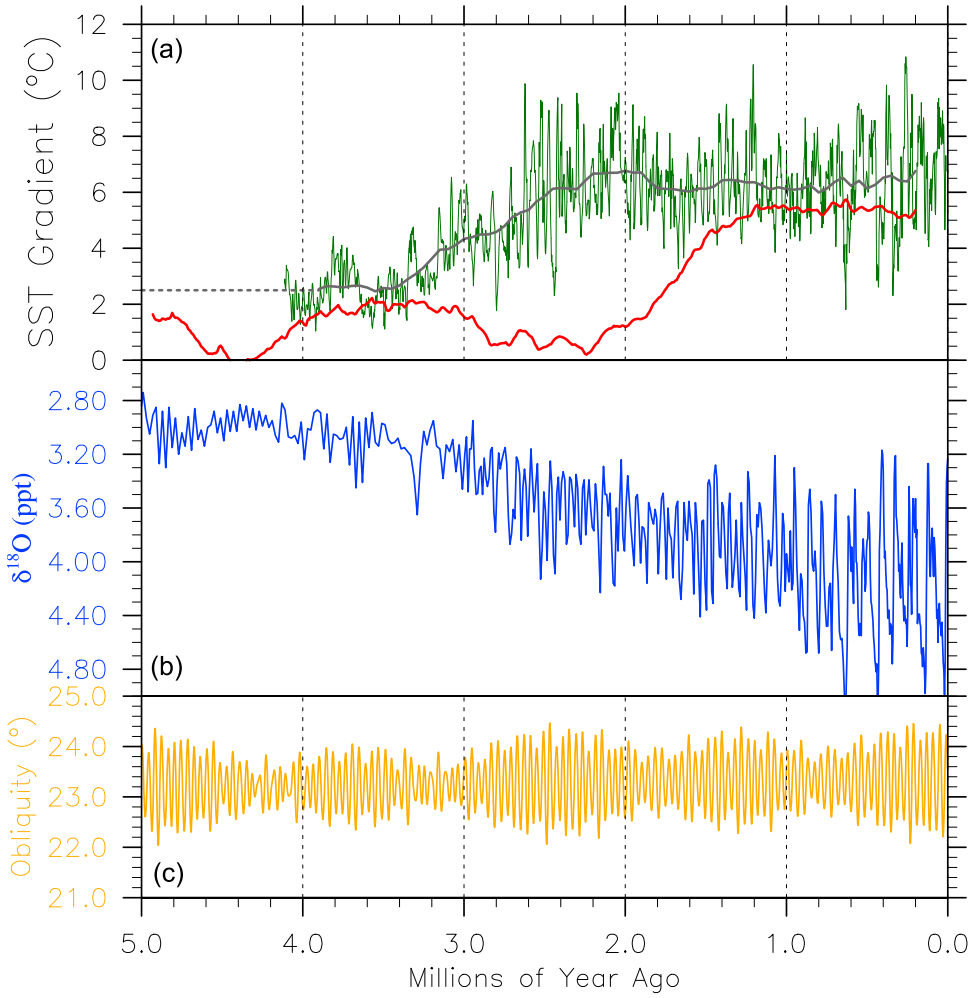

Figure 1. Evolution of climate over the past 5 Myr. (a) The development of the meridional sea surface temperature (SST) contrast in the tropical east Pacific (green line, from *Brierley et al.* [2009]) and the zonal SST gradient along the equator (red line, from *Wara et al.* [2005]). The meridional temperature difference is estimated from alkenone records from the ODP sites 846 (3°S, 91°W) and 1012 (32°N, 118°W). The zonal temperature difference is calculated from Mg/Ca temperature records from ODP sites 806 (0°N, 159°E) and 847 (0°N, 95°W). The black and the red lines are obtained using a 400,000 year running mean. (b) The oxygen isotope record (blue line, from *Lisiecki and Raymo* [2005]) shows a general cooling of the climate since 5 Ma and an increase in variability associated with glacial cycles. (c) The variations of Earth's obliquity, a key component of the orbital forcing that drives glacial cycles, are shown by the orange line and appear throughout the δ^{18}O record [*Laskar et al.*, 2004].

potential factor in the onset of glacial cycles, especially changes in the tropics and subtropics [*Philander and Fedorov*, 2003; *Barreiro et al.*, 2006; *Fedorov et al.*, 2006; *Huybers and Molnar*, 2007]. Estimates of Pliocene SSTs have become more numerous and accurate in the past few years, leading to new insights into the warm climate state before the onset of Northern Hemisphere glaciation [*Dowsett and Robinson*, 2009] and the subsequent climate evolution. For example, there have been dramatic changes in tropical SST gradients over the past ~5 Myr (Figure 1) in both the zonal gradient along the equator (red, after *Wara et al.* [2005]) and the meridional gradient on the eastern side of the Pacific (green, after *Brierley et al.* [2009]). Both these records are created as the difference between 2 ocean cores: for this study, we take them to be representative of the basin-wide situation as suggested by *Wara et al.* [2005] and *Brierley et al.* [2009]. Uncertainties in this interpretation are covered later in the discussion section.

[6] Early Pliocene Pacific SSTs were zonally uniform along the equator, so that the equatorial cold tongue was either nonexistent or very weak [*Philander and Fedorov*, 2003; *Wara et al.*, 2005; *Fedorov et al.*, 2006]. This state has been dubbed a "permanent El Niño-like state" or "permanent El Niño" [e.g., *Molnar and Cane*, 2002; *Philander and Fedorov*, 2003], which implies only that the mean ocean state had a minimal zonal temperature contrast

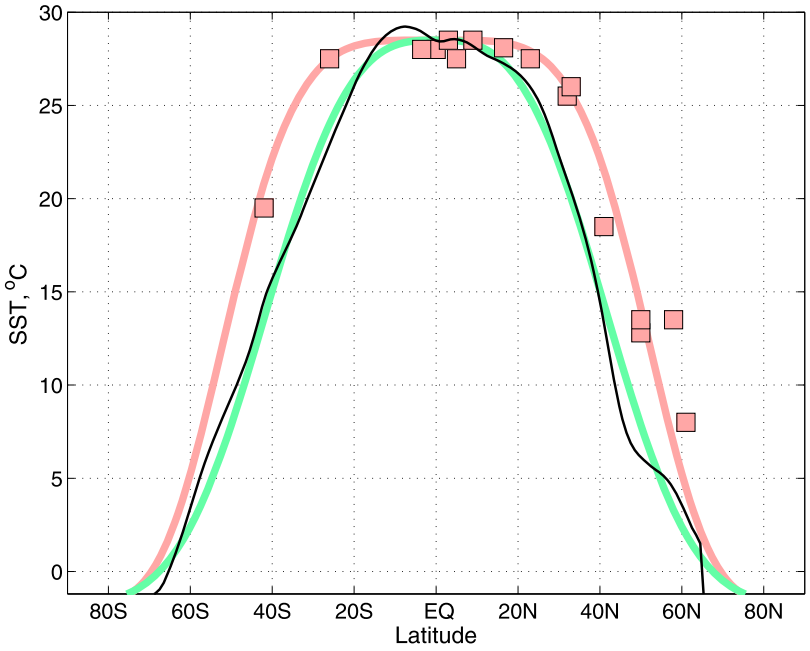

Figure 2. Meridional SST profiles used for the simulations. The early Pliocene SST distribution (~4 Ma) in the mid-Pacific (pink squares), after *Brierley et al.* [2009] with an addition of a data point at 16°37′N, 59°47′E [*Huang et al.*, 2007]. The pink line shows the hypothetical fit of equation (1) to the proxy data. The black line shows the modern climatological SSTs along 180°E from *Rayner et al.* [2003]; the green line shows the hypothetical fit to the modern dateline SSTs also based on equation (1) but with different coefficients. The two fitted lines are used as the boundary conditions for the meridional SST gradient experiments. We expect the error bars in this reconstruction to be of the order of 1°C or smaller, even though more accurate estimation will have to wait until more data are available. Errors would emerge from (1) the adjustments of temperatures, (2) systematic errors in alkenone and Mg/Ca methods, and (3) uncertainties due to temporal variations in temperatures within the time interval considered.

along the equator rather than saying anything about the climate variability. Further discussion of the nature of permanent El Niño exists elsewhere in the literature [e.g., *Fedorov et al.*, 2006; *Fedorov et al.*, 2010; *Brierley et al.*, 2009; *Bonham et al.*, 2009]. Such climate states appear to have existed earlier in the Cenozoic as well, but their termination was not linked to an onset of glacial cycles, probably due to higher CO_2 than in the Pliocene [*Nathan and Leckie*, 2009].

[7] Recent data indicate that the Pliocene meridional SST gradient between the equator and the subtropics was also very weak, roughly 2°C around 4 Myr ago [*Brierley et al.*, 2009]. Thus, the early Pliocene had a vast pool of warm water encompassing the whole extent of the tropics rather than just zonal uniformity along the equator implied by the term "permanent El Niño." Midlatitudes and subpolar regions were also significantly warmer. This is supported by a recent early Pliocene SST reconstruction (Figure 2) [after *Brierley et al.*, 2009], which shows a very flat SST distribution in the tropics and midlatitude and subpolar latitude warmer on average 3°C–6°C. Because of uncertainties in the paleodata, here we define the warm pool simply as waters with temperatures above a set threshold rather than using a dynamical definition, such as that of *Lindzen and Nigam* [1987].

[8] The gradual contraction of the warm pool toward the equator (and the overall increase of the meridional SST gradient, Figure 1) clearly began before the date of 2.7 Ma given for the onset of Northern Hemisphere glaciation [*Haug et al.*, 1999] and continued after that date. The meridional temperature gradient on the eastern side of the Pacific appears to have reached its modern values around 2 Ma; the zonal SST gradient along the equator appears to have reached its modern values at a somewhat later time. (It is possible that the meridional gradient in the ocean interior reached modern values roughly at the same time as the zonal gradient, but in the absence of actual data from the mid-ocean we use 2 Ma as the tentative threshold.)

[9] Using an atmosphere general circulation model, *Barreiro et al.* [2006] investigated the effect of a permanent El Niño-like state on global climate and showed that such a climate state in the tropics could help maintain an ice-free Northern Hemisphere. *Huybers and Molnar* [2007] used recent observations to determine the impact of a composite El Niño event on North American climate. They concluded that El Niño events can cause a warming of high northern latitudes and, therefore, additional ice melt. Their analysis suggested that the impact of insolation changes caused by obliquity variations is less than the impact of an El Niño and, hence, of permanent El Niño conditions. On the other

hand, *Haywood et al.* [2007] forced a coupled climate model to produce a permanent El Niño in the equatorial region but found no significant impacts to the ice growth over Greenland. These studies did not account for a potential role of changes in the meridional SST gradient. For example, *Barreiro et al.* [2006] explicitly assumed that the meridional SST distribution matched that of the present-day. Thus, the question of the relative importance of the two SST gradients becomes critical for understanding climate evolution since the early Pliocene.

[10] The aim of the present study is to investigate whether the variations in the meridional SST profile seen since the early Pliocene were conducive to Northern Hemisphere glaciation and how these variations compare to the effects associated with zonal SST variations. We treat the two gradients as completely independent, although in reality there should be a connection between them. *Brierley et al.* [2009] looked at the combined tropical effects of these changes (which include a slowdown of the atmospheric Hadley circulation). Here, we concentrate on the relative roles of the changes on climatic processes on land (including temperatures and snowfall over northern high latitudes and climate conditions over Africa and parts of Asia).

[11] The effects of altered equator-to-pole temperature gradients have long been a focus of paleoclimate studies [e.g., *Barron*, 1987; *Caballero and Langen*, 2005], as well as studies of the response of atmospheric models to different forcing [e.g., *Neale and Hoskins*, 2000; *Brayshaw et al.*, 2008]. Many of those studies use atmospheric general circulation models to determine the response to imposed SSTs. In this paper, we build upon this approach and explore how Pliocene-Pleistocene climate evolution is affected by changes in two key properties of the climate system: the meridional SST gradients from the equator to the subtropics to midlatitudes and the equatorial zonal SST gradient.

2. Method

[12] These experiments use the Community Atmosphere Model, version 3 (CAM3) at T85 resolution [*Collins et al.*, 2006]. We repeated calculations with a lower-resolution version of the model (T42) and found only minor differences between the two versions. The model was developed at the National Center for Atmosphere Resolution (NCAR) as part of their coupled climate model that was included in the International Panel on Climate Change's fourth assessment report and is used broadly for paleoclimate studies [e.g., *Caballero and Langen*, 2005; *Brierley et al.*, 2009]. The majority of the boundary conditions are identical to the present-day control simulation of *Collins et al.* [2006]. We emphasize that the goal of this study is not to reproduce accurately the climate conditions of the early Pliocene and subsequent glaciation but rather to investigate the gross effects of changes in the meridional and zonal SST gradients and their relative roles; hence, our use of the modern orography and land surface boundary conditions.

[13] The present study builds on the approach of *Barreiro et al.* [2006], who explored the early Pliocene climate in an atmospheric global climate model. They specified an idealized permanent El Niño state in the tropics (between 30°N and 30°S) by zonally extending the modern meridional SST profile from the dateline. Thereby, all zonal SST gradients in the tropics were eliminated, but the meridional gradients were left unchanged.

[14] Similarly, we will contrast and compare three idealized experiments: (1) the early Pliocene experiment with reduced meridional and no zonal SST gradients, (2) the experiment with the modern meridional SST gradient but no zonal SST gradient (the "modern zonal"), and (3) the present-day experiment forced by the modern SST distribution at the surface (the "modern control"). All these experiments have the same amount of atmospheric CO_2 (the 1990 level of 355 ppm), the same orography and land surface, but different imposed sea surface conditions (SST and sea ice coverage).

2.1. Early Pliocene Simulation

[15] The forcing for the early Pliocene simulation is obtained by zonally extending the SST profile from the Pliocene reconstruction shown in Figure 2 with several modifications as described below. For details of this reconstruction, see *Brierley et al.* [2009]; an extra point was added at around 16°N using data from the Arabian Sea [*Huang et al.*, 2007]. This reconstruction for the mid-Pacific SSTs was created by incorporating adjusted proxy data mostly from the North Atlantic to represent a Pacific oceanographic setting. Since typical temperatures in the North Atlantic are warmer than in the Pacific, for the Atlantic Ocean, we use a slightly altered meridional SST profile but still with no zonal gradients across the basin.

[16] The chosen period of the reconstruction, around 4–4.2 Ma, coincides with the time when the east-west temperature gradient along the equator almost collapsed and the meridional temperature gradient was minimal (Figure 1a). Further, it is assumed that the zonal temperature gradients within each basin were absent (except in the South Pacific, see below), which is an oversimplification but allows the impacts of the changes in meridional gradient to be isolated.

[17] The analytical expression for the SST profile is obtained by fitting the following exponential function to the temperature estimates in Figure 2:

$$T(\theta) = (T_{\max} - T_{\min}) \exp\left[-\frac{1}{a}\left(\frac{|\theta|}{45}\right)^N\right] + T_{\min} \qquad (1)$$

where θ is the latitude in degrees, $T_{\min}$ is the temperature of freezing for seawater (set to −1.8°C), and $T_{\max}$ is the maximum temperature in the tropics (set to 28.5°C for all profiles). The fitting parameters N and a control the strength of the extratropical SST gradient and the curvature of the SST profile near the equator. For the early Pliocene Pacific, N is set to 4.5, while the constant a was determined to be 2.6 by a least squares fit to the temperature estimates [*Brierley et al.*, 2009]. To simulate the warmer temperatures in the North Atlantic, the value of a is set to 4.2.

[18] There are some marked similarities between equation (1) and the theoretical result of *Emanuel* [1995] obtained for a heating source at the equator. Accordingly, the high value of N indicates that the system is a long way from the critical

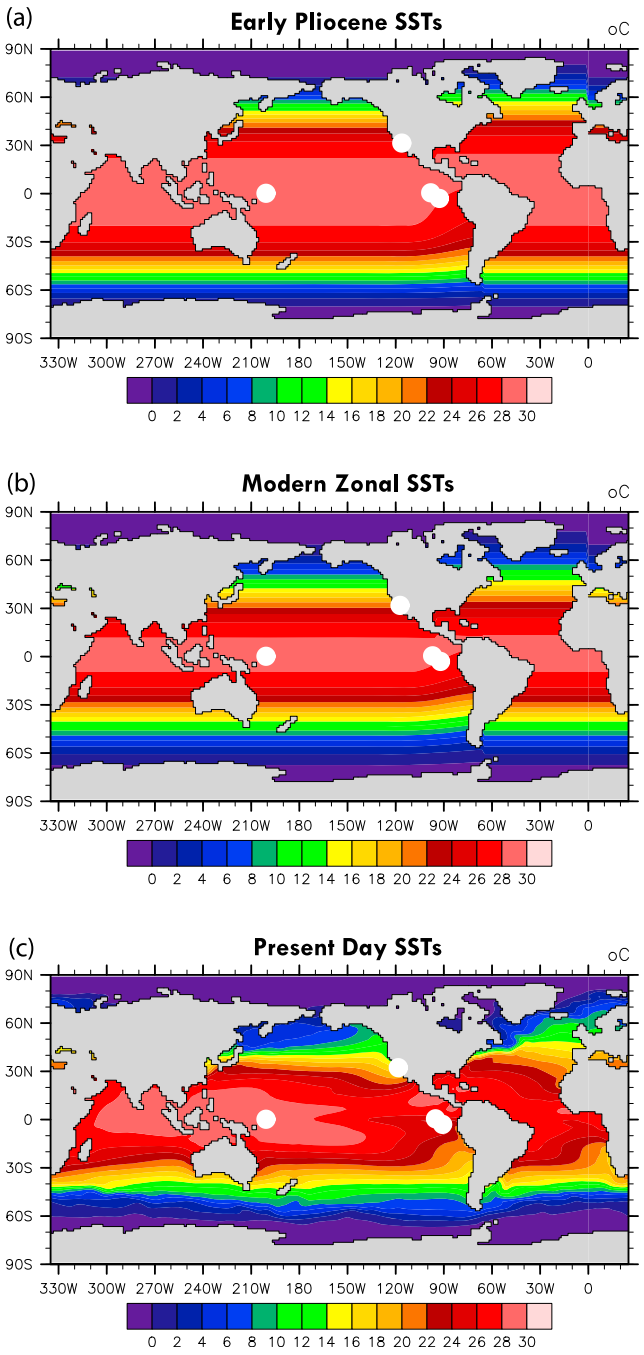

Figure 3. Annual mean sea surface temperature fields for the three experiments. White circles show the locations of the ODP cores used to determine the evolution of zonal and meridional SST gradients in Figure 1.

value to initiate meridional monsoonal circulations [*Plumb and Hou*, 1992]. Indeed, the early Pliocene simulation does not exhibit an Asian monsoon (see section 3.5).

[19] The early Pliocene SST profile as derived from equation (1) is shown in Figure 2 (pink line), along with the originating data. To simulate the seasonal cycle, this profile is shifted each month along the meridian, matching the progression of the modern annual cycle. To take into account the effect of the Peru Current along the coast of South America, which was warmer in the early Pliocene but still colder than the surrounding waters [*Dekens et al.*, 2007], a cold temperature anomaly was added to the SST field. The SSTs constructed in this manner are shown in Figure 3a. The fractional sea ice cover is calculated from the SST. There is no sea ice for SSTs warmer than 0.8°C, and the fractional coverage increases linearly until −1.8°C, which is assumed to have complete sea ice coverage.

[20] Thus, this simulation uses the early Pliocene SST reconstruction described above with the imposed meridional SST profile from Figure 2 and the assumption of zonal uniformity (with the exceptions that the North Atlantic is warmer and the Humboldt Current is colder than this profile). The early Pliocene simulation is similar to that performed by *Brierley et al.* [2009], but here, the orography and land surface conditions are specified at present-day conditions. This simulation will henceforth be termed the "early Pliocene" run.

2.2. Modern Zonal Simulation

[21] The second simulation uses the fit to the modern meridional SST profile shown as the green line in Figure 2. The method is identical to the early Pliocene run except for the coefficients used to create the hypothetical SST profile and the imposed sea ice coverage (a function of the SST). This simulation is termed a "modern zonal" run because all major zonal SST variations within each ocean basin are eliminated.

[22] The same equation (1) is used to create a zonally uniform version of modern conditions, but with N set to 3 and a set to 1.2 (1.7 for the North Atlantic). This meridional profile fitted to modern conditions is shown by green line in Figure 2, and the annual mean SST pattern is shown in Figure 3b.

[23] This experiment is generally similar to the study of *Barreiro et al.* [2006] with a few exceptions. First, our modern zonal SST field assumes zonally uniform in the extratropical oceans (removing the effects of boundary currents), while *Barreiro et al.* [2006] use modern observations in the extratropics that are joined to the zonally uniform tropics via linear interpolation. Second, *Barreiro et al.* [2006] use the Geophysical Fluid Dynamics Laboratory AM2.0 model, whereas we use NCAR's CAM3. Third, *Barreiro et al.* [2006] made some alterations to the land surface and orography for their Pliocene simulations.

[24] Note that because of the way they are defined, the two meridional SST profiles in Figure 2 have the same temperature at the poles, so that any potential changes in temperatures over the polar regions are minimized, which should emphasize the effects of SST changes from the tropics to midlatitudes. Because of this issue, and for the purposes of this study, we define the meridional SST gradient as temperature difference from the equator to, say, 50° of latitude, rather than the equator-to-pole difference. Also, to approximate the climate of circa 2 Ma by which time the meridional gradient is fully developed, we use the modern zonal experiment: we assume that meridional SST changes

between 2 Ma and the present are relatively minor compared to those between 4 and 2 Mar.

2.3. Modern Control Simulation

[25] The third simulation uses a modern SST and sea ice climatology based on the average of 1961–1990 taken from the HadISST data set [*Rayner et al.*, 2003]. It is similar to the control run of *Collins et al.* [2006] but shall be termed the "modern control" run in this paper.

3. Results

3.1. Increase of Meridional SST Gradient

[26] First, we explore how climate conditions over land in the Northern Hemisphere are affected by the increase in the meridional SST gradient between the early Pliocene and modern zonal simulations (Figure 4). There is a dramatic reduction in both winter and summer surface air temperatures (Figures 4a and 4b, respectively) throughout the Northern Hemisphere, in the range of 4°C–8°C.

[27] There is a strong change in surface temperatures in northwest Canada in boreal winter, where the increase in the meridional SST gradient causes more than 5°C of cooling. However, the average temperature of this region in winter is already below the freezing point in the early Pliocene simulation. Any additional cooling will likely not impact the persistence of the snowpack, as there is already very little melt occurring in that region during winter. On the other hand, substantial areas of North America see reductions in the summer air temperature, which would act to prolong the existence of the winter snowpack. The drop in summer temperatures is caused by increased mid- and low-level cloud cover over the continent, which reduces the amount of incoming solar radiation reaching the surface. This increase in cloud cover is, in turn, caused by a strengthening of the midlatitude jet stream, associated with the increased meridional SST gradient and thermal wind balance.

[28] To determine the impact of changes in the meridional SST distribution on ice buildup, one can consider factors that would influence an ice sheet's mass balance. An ice sheet will grow over a year if it gains (accumulates) a greater amount of ice than is removed (ablated). The accumulation of ice is relatively easy to determine from the simulations, as it is equal to the liquid water equivalent of the total amount of snow falling over the year. The ablation is harder to diagnose, as it requires knowledge of such properties as the surface albedo, rainfall, and temperature of the ice. A simple, frequently used parameterization of the ablation is the positive degree day approach [*Greuell and Genthon*, 2004]. This method assumes that the amount of ablation is directly proportional to the sum of all daily mean temperatures above freezing (positive degree days). Therefore, the change in ice sheet mass balance can be expressed as

$$dM/dt = A - \beta \times \mathrm{PDD} \tag{2}$$

where M is the mass of the ice sheet (kg), t is time, A is the total annual snowfall in liquid water equivalence (kg), β is the degree day factor, and PDD is the annual amount of positive degree days (°C day). The product $\beta \times$ PDD describes the actual or potential annual loss of snow/ice by ablation. Estimates for the degree day factor range from 3 to 15 mm d^{-1} $°C^{-1}$ [*Braithwaite and Zhang*, 2000].

[29] There is a reduction in the number of positive degree days throughout the Arctic caused by the transition to the colder meridional SST distribution, which becomes stronger toward midlatitudes (Figure 4c). The reduction in positive degree days would act to increase the persistence of snow cover during the melt season. There is a reduction in the total amount of snowfall over the year in the Arctic and an increase below ~70°N (Figure 4d). This arises from a reduction in moisture transport to the high latitudes, caused by the storm tracks occurring farther south.

3.2. Increase of Zonal Tropical SST Gradient

[30] To determine the consequences of the establishment of zonal SST gradients in the tropics over the past 2 Myr, we look at the differences between the modern control and the modern zonal simulations (Figure 5). There is a notable decrease in winter temperatures throughout Canada especially around the Hudson Bay. The summer impacts include a broad warming of the interior of North America of more than 4°C (generally consistent with the results of *Barreiro et al.* [2006]). This is a consequence of an increase in the upper level subsidence over the continent, leading to a suppression of clouds and a subsequent increase in incoming solar radiation hitting the surface. In the present climate, cold La Niña events lead to a summer warming and drying of the Great Lakes region [*Green et al.*, 1997]. In our simulations, we see a much stronger signal throughout North America. This is not surprising since the applied tropical SST anomaly is much larger and longer in duration than observed under a typical La Niña. In the annual mean (not shown), we see a cooling of Canada and a warming of the interior of the United States. The cooling is dominated by the winter temperature pattern, and the warming is dominated by the summer changes.

[31] The warming over the U.S. interior leads to an increase in positive degree days there, associated with the establishment of tropical zonal SST gradients. However, there is a reduction in positive degree days in northern Quebec and Labrador, which is an important area for ice sheet growth (coinciding with the probable origin of the Laurentide Ice Sheet). Similarly, there is an increase in total annual snowfall in Alaska (associated with deepening of the Aleutian low) as well as some changes over Greenland. However, there is large uncertainty about how much ice existed on Greenland, and therefore its elevation, in the Pliocene [*Lunt et al.*, 2008]. These simulations have all been performed with modern orography, so any results over Greenland should be treated with caution.

[32] The pattern in Figure 5c shows an increase in positive degree days over the interior of the U.S., which does not agree with the conclusion of *Huybers and Molnar* [2007], who used present-day observations to determine the impact of El Niño events on the positive degree days over North America. There are a number of factors that may explain this difference, of which the most probable cause is the methodology of *Huybers and Molnar* [2007]. Positive degree days is a diagnostic that emphasizes the summer changes

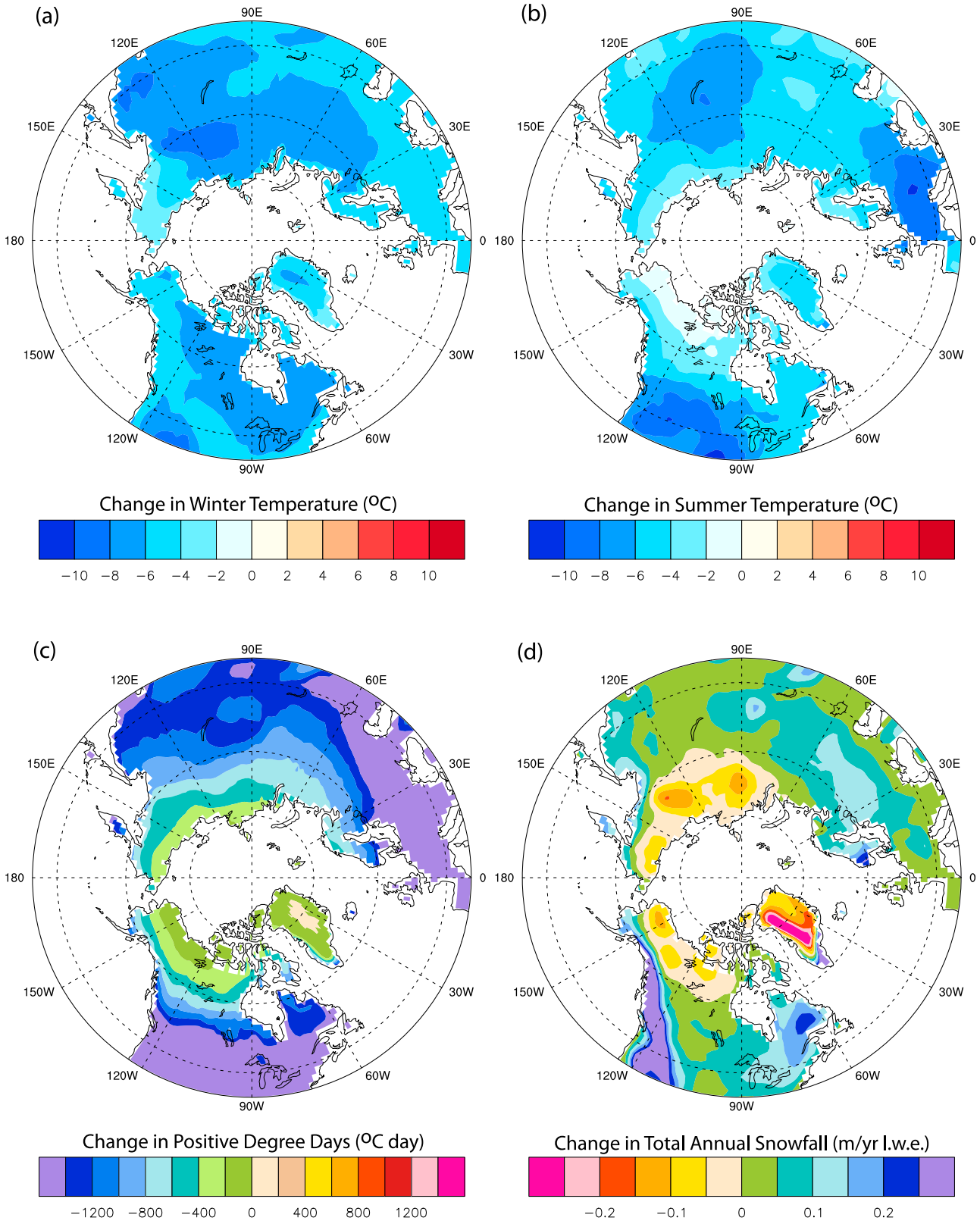

Figure 4. Impacts of the increase in the meridional SST gradient since the Pliocene on the northern high latitudes. (a and b) Changes in winter (DJF) and summer (JJA) average surface temperature suggesting hemisphere wide cooling, in °C. (c) Changes in positive degree days, in °C days and (d) in total annual snowfall, in m yr^{-1} of liquid water equivalent.

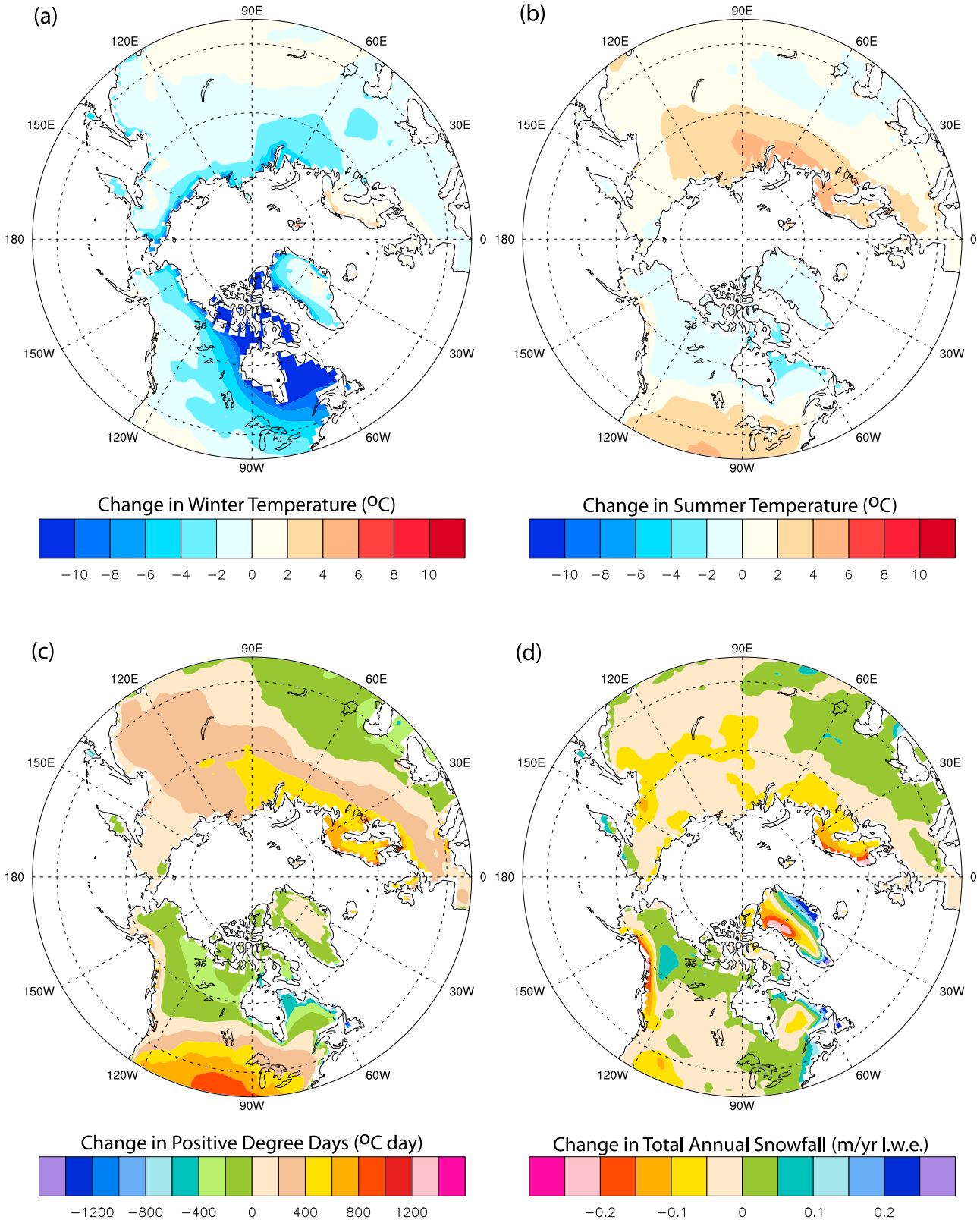

Figure 5. Same as Figure 4 except for impacts of establishing modern zonal SST gradients in the tropics on the northern high latitudes.

(since most melt occurs in summer). However, the pattern of *Huybers and Molnar* [2007] does not appear to show any signature of the observed summer warming over land during El Niño [*Green et al.*, 1997; *Deser et al.*, 2006]. Therefore, the results of *Huybers and Molnar* [2007] are probably biased toward winter, when modern, transient El Niño events reach their peak. Thus, the climate response to a permanent change in SST can differ in a number of respects from the response to interannual and seasonal changes [*Haywood et al.*, 2007].

3.3. SST Changes and Ice Sheet Growth

[33] The analysis above shows that the changes in tropical SST gradients since the early Pliocene would have impacted the buildup of snow in North America. The positive degree days and snow accumulation presented previously can be combined to create a single measure for the ice sheet mass balance. Although this method alone cannot determine whether these changes are sufficient to allow glacial inception, it permits quantitative comparison of the two gradient contributions to the onset of Northern Hemisphere glaciation. In order to create this single measure, we return to equation (2) and set the degree day factor, β, to be 5 mm d^{-1} $°C^{-1}$. This is a value typical of late season snow cover [*Braithwaite and Zhang*, 2000], and a snowpack surviving throughout the melt season is a necessary precursor to the growth of an ice sheet. This allows estimation of the potential ice sheet mass balance (dM/dt) over the course of 1 year (Figure 6).

[34] Greenland is the only region in the Northern Hemisphere for which this metric is positive in the modern control (the coldest of the runs presented). This implies that favorable conditions for growing or sustaining an ice sheet exist only over Greenland in the modern climate. The majority of Canada has values of -5 m yr^{-1} or less, meaning that an extra 5 m of water must fall as snow each year (at least 15 m of actual snow) to start developing an ice sheet. This is an order of magnitude above the present snow fall.

[35] It must be reiterated that Figure 6a shows only potential ice sheet mass balance (dM/dt in equation (2)), since potential melt, calculated as the positive degree days multiplied by the degree day factor in equation (2), is the dominant term over North America. The values of potential melt over much of the region far exceed the annual snowfall.

[36] Overall, the establishment of meridional SST gradients has a stronger effect than zonal SST changes in the tropics. The increase in the meridional gradient by itself results in an increase in ice sheet mass balance of up to 10 m yr^{-1} in high-latitude North America (Figure 5b). The establishment of the zonal tropical SST gradient causes an increase of 1–2 m yr^{-1} poleward of 50°N, with the largest increase over northwest Canada. Both increases are mostly due to the temperature changes over land (and hence changes in positive degree days). If a β parameter appropriate for ice rather than late season snow was used, changes in positive degree days would dominate the total annual snowfall even more.

[37] One advantage of presenting the data as changes in ice sheet mass balance is that climate models have too low a resolution to accurately grow an ice sheet over sharp topography (such as a mountain). However, data from climate models are regularly downscaled to drive separate ice sheet models because trends in the simulated mass balance are thought to be much more reliable.

3.4. Impacts of Changes in the SST Gradients on Clouds and Atmospheric Water Vapor

[38] The transition from the warm early Pliocene to colder climate conditions evidently resulted in dramatic changes in the mean global temperature. Our numerical experiments suggest that the mean global temperature decreases by 3.2°C between the early Pliocene and modern zonal simulations and decreases by 0.6°C between the modern control and modern zonal runs (Table 1). This suggests that the early Pliocene global mean temperature was ~4°C higher than the modern climate and possibly higher still as our analysis is likely to underestimate temperature changes in high latitudes. Previous estimates indicated up to 3°C warmer temperatures for the mid-Pliocene [*Ravelo et al.*, 2004; *Haywood and Valdes*, 2004].

[39] The global cooling implies a reduction in the blackbody longwave emission from the Earth's surface. All the simulations were integrated until quasi-stable equilibrium was reached, so the reduction in emitted longwave radiation must be balanced by other radiative changes. These radiative changes are largely from water vapor and cloud changes (Table 1), which is consistent with the conclusions of *Barreiro et al.* [2006] and *Brierley et al.* [2009]. However, the increase in the meridional SST gradient results in a much greater role of water vapor for the radiation balance. Establishment of zonal SST gradients has a smaller impact because the drying in the Southern Hemisphere is partially compensated by the moistening associated with the intensification of the (northern) Intertropical Convergence Zone (ITCZ).

Figure 6. Potential ice sheet mass balance. (a) Potential ice sheet mass balance (dM/dt) in the modern control simulation as calculated by equation (2). (b) Changes in the potential mass balance associated with the increase in the meridional SST gradient seen between 4 and 2 Ma. Mass balance shifts to positive values (indicative of potential ice sheet growth) almost everywhere in North America. (c) Changes in the mass balance associated with the termination of permanent El Niño conditions and establishment of tropical zonal SST gradients. Mass balance shifts to positive values in the northern regions of North America. Note the nonlinear scale. All changes are calculated from the fields presented in the Figures 4 and 5. The value of β parameter is set to 5 mm of melt per positive degree day. Changes in the mass balance are largely due to summer temperatures. Note that our results for Greenland in Figures 6b and 6c should be treated with caution, since we kept the modern surface elevation.

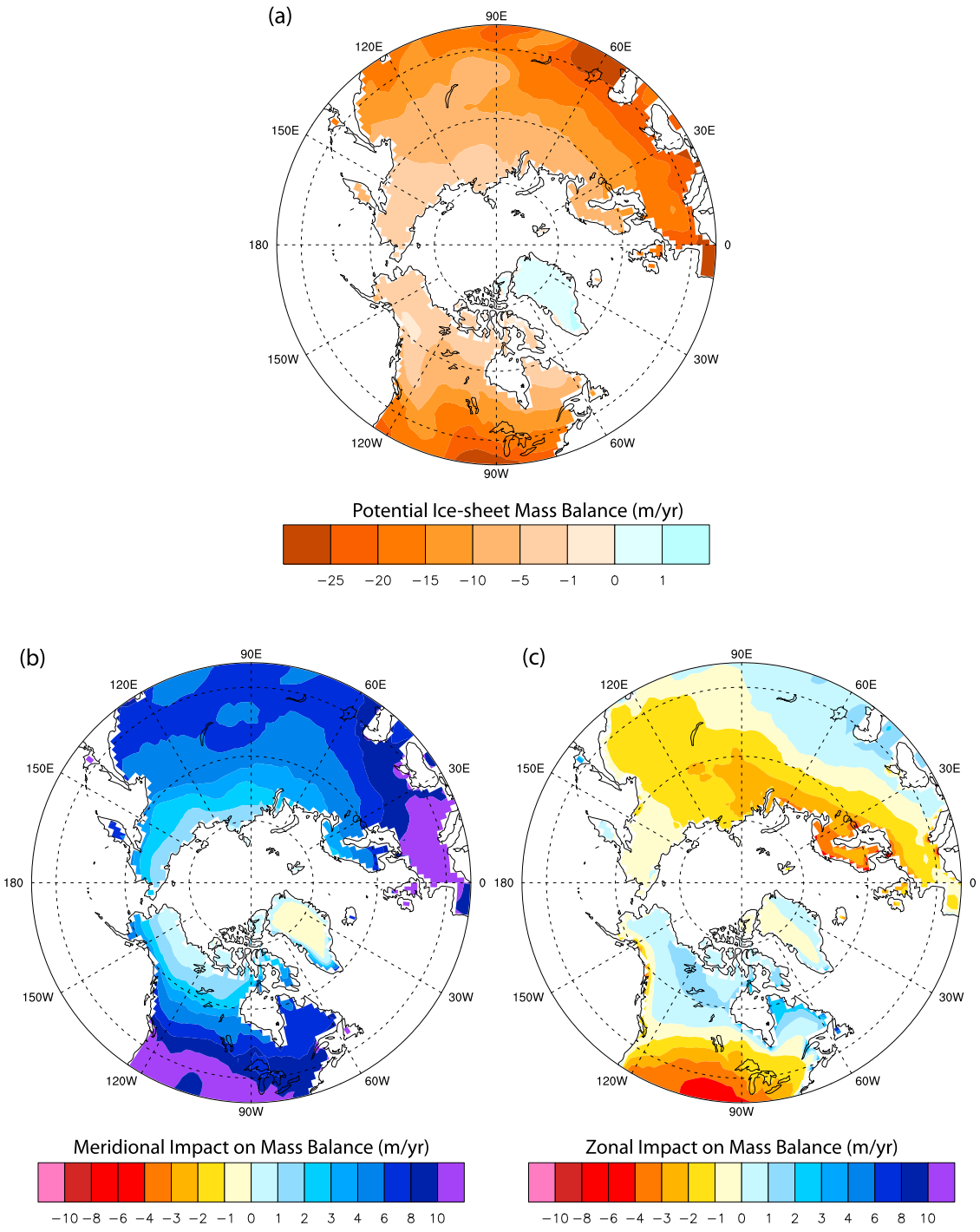
(a)
90E
120E
60E
150E
30E
180
0
150W
30W
120W
60W
90W
Potential Ice-sheet Mass Balance (m/yr)
−25 −20 −15 −10 −5 −1 0 1
(b)
Meridional Impact on Mass Balance (m/yr)
−10 −8 −6 −4 −3 −2 −1 0 1 2 3 4 6 8 10
(c)
Zonal Impact on Mass Balance (m/yr)
−10 −8 −6 −4 −3 −2 −1 0 1 2 3 4 6 8 10

Figure 6

Table 1. Global Mean Changes in Surface Temperature Arising From the Increase in Meridional and Zonal SST Gradients in the Atmospheric Global Climate Model[a]

	Meridional SST Gradient	Tropical Zonal SST Gradient
Global mean temperature change (°C)	−3.2	−0.6
Combined water vapor and lapse rate effects (W m^{-2})	−10.8	−2.6
Total cloud effect (W m^{-2})	−3.1	−2.7
Surface albedo effect due to changes in snow and sea ice cover (W m^{-2})	−1.8	−2.7

[a]Main components of the atmospheric radiative that contributes to those changes are also shown. Positive is defined as directed toward the Earth for the heat fluxes, so that negative numbers indicate a greater energy loss to space. Note that changes in heat fluxes related to surface albedo should be treated with caution since we do not have interactive ice sheets.

[40] The impact of the meridional SST gradient on the water vapor latitudinal distribution (Figure 7) is very similar to that found by *Brierley et al.* [2009], who included orography and land surface changes in their early Pliocene simulations. There is an increase in water vapor near the equator associated with increased atmospheric deep convection. The decrease elsewhere is a consequence of the decreased temperatures and the Clausius-Clapeyron relationship.

[41] The water vapor changes from establishing zonal SST gradients occur primarily in the tropics. There is a suppression of deep convection and a cooling over the upwelling zones in the Southern Hemisphere, leading to a local decrease of water vapor content. A slight increase in the vertical water vapor transport in the northern tropics leads to a positive anomaly above 700 mbar and a negative anomaly below. This is associated with the strengthening of the ITCZ in the Northern Hemisphere.

[42] The changes in water vapor are accompanied by cloud cover changes in the atmosphere (Figure 8). The increase in meridional SST gradient leads to an increase in high cloud cover in the tropics and a reduction in the subtropics. This is associated with a strengthening of the Hadley circulation by roughly 30% [*Brierley et al.*, 2009]. The largest cloud changes caused by the establishment of zonal SST gradients are related to the suppression of deep convection and the establishment of stratus decks over the Southern Hemisphere tropical upwelling zones, especially the Peru-Chile current system. There is an increase in high cloud cover around 10°N associated with the strengthening of deep convection in the ITCZ region and a strengthening of the South Asian monsoon circulation (discussed more later). Part of the decrease in low-level cloud cover in the Arctic arises from shifts in the edge of sea ice in the Barents Sea associated with prescribed changes in SST.

[43] For the global mean, increasing either meridional or zonal SST gradients leads to less greenhouse forcing of the cloud cover, with a reduction in high, warming clouds and an increase in low, cooling clouds. The magnitudes of the global mean cloud changes are similar for both experiments

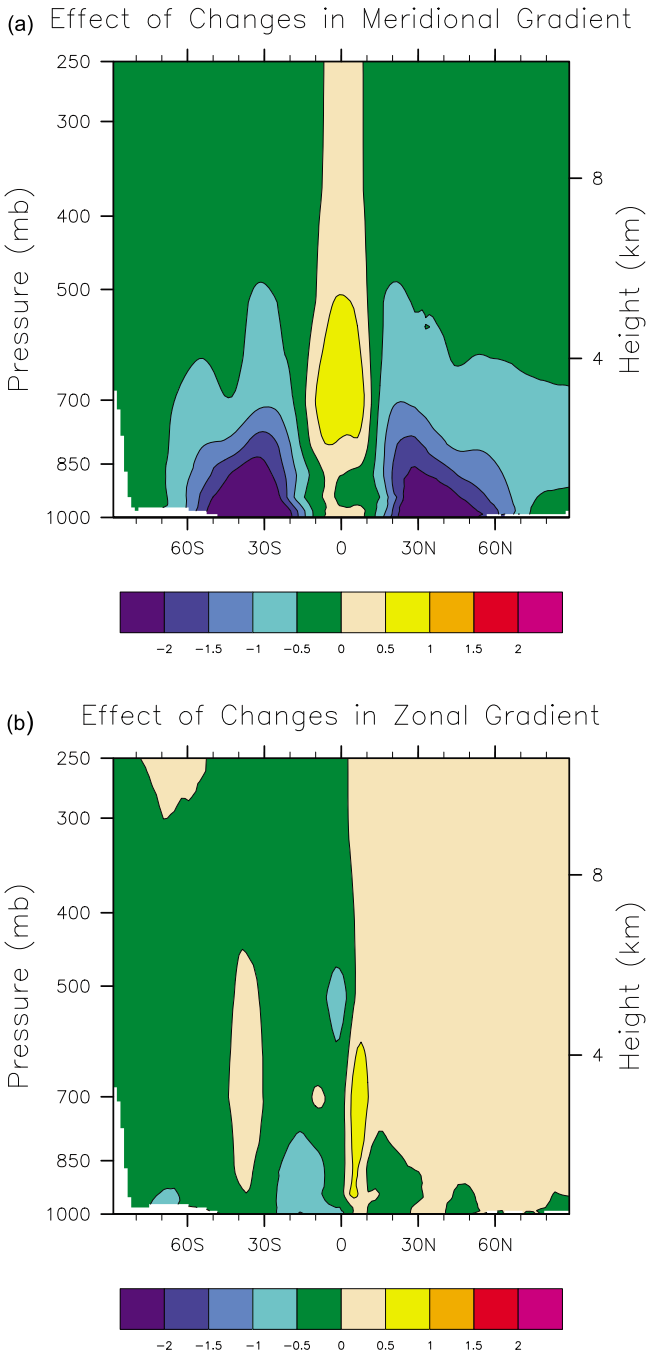

Figure 7. Changes in the latitudinal distribution of the zonally averaged water vapor content of the atmosphere, in g kg^{-1}, caused by increasing (a) meridional SST gradient and (b) zonal SST gradient in the tropics. The overall reduction in water vapor, which is greater for Figure 7a, arises from the reduced sea surface temperatures and the Clasius-Clapeyron relationship. The increases in water vapor concentrations in the narrow equatorial regions are associated with increased deep convection.

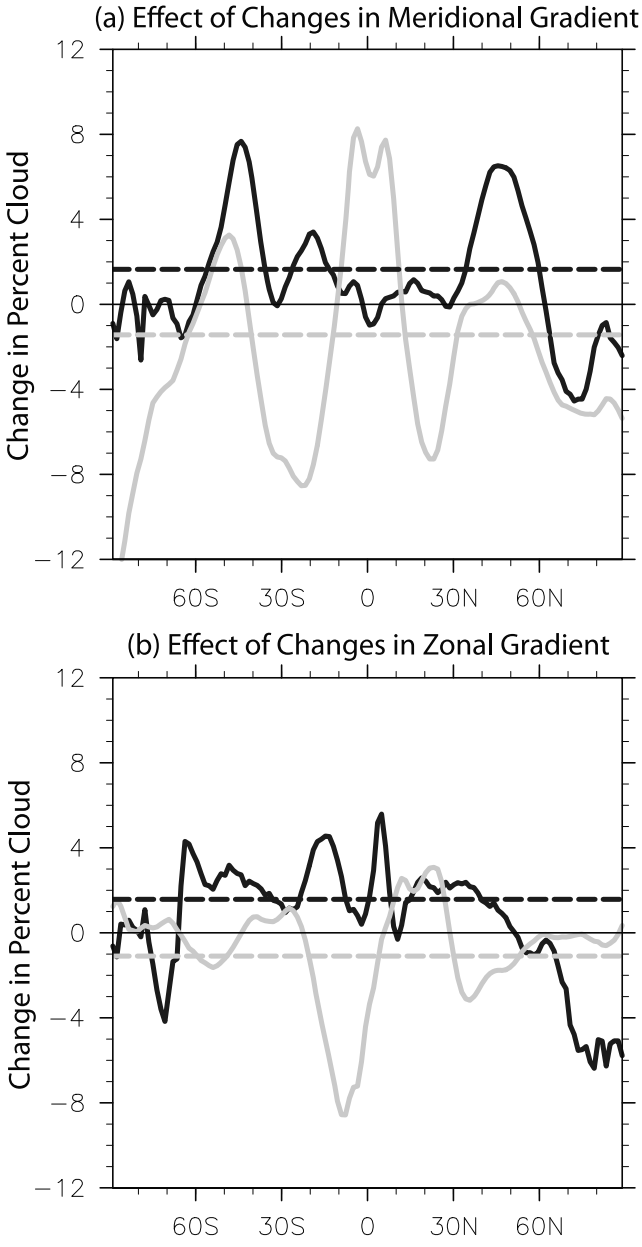

Figure 8. Changes in the zonally averaged distribution of low and high clouds (black and gray lines, respectively) as a consequence of increasing (a) meridional SST gradient and (b) zonal SST gradient in the tropics. High clouds are defined as clouds above the 400 mbar pressure level, while low clouds occur below 700 mbar. Cloud cover is measured in percent of the total area. The dashed lines indicate global annual mean changes. While latitudinal distribution of changes in the cloud cover is different in each case, the mean changes are comparable: an increase in highly reflective low clouds and a reduction in greenhouse high clouds.

as are the radiative impacts of those changes (Table 1 and Figure 8).

3.5. Impacts of Changes in SST Gradients on Precipitation Over Land in the Tropics

[44] An important element of the climate evolution over the Pliocene-Pleistocene involves climate changes in Africa [e.g., *deMenocal*, 2004] and over India [e.g., *Huang et al.*, 2007]. In fact, the aridification of East Africa in the Pliocene-Pleistocene is thought to be a driver for hominid evolution [*deMenocal*, 2004]. To investigate these issues, we look at the simulated precipitation minus evaporation (P - E) over Africa and surrounding regions (Figure 9). As tropical rainfall has a strong seasonality, we consider boreal summer (June, July, and August, JJA) and winter (December, January, and February, DJF) separately. It is worth reiterating here that the land cover has been specified as identical to the modern for all simulations, so no vegetation feedbacks can exist in these runs. Those feedbacks would amplify any moisture changes in the area by affecting evaporation from the land surface. Also, the orography is identical in all the simulations, which has been shown to impact the climate of East Africa [*Sepulchre et al.*, 2006].

[45] The establishment of modern meridional gradients leads to a summer drying stretching from North Africa to northern India and a winter drying in the Sahel and over the Arabian Sea. The summer North African signal comes from a reduction in the poleward extent of the West African monsoon. In the early Pliocene simulation, the Hadley circulation is relatively weak and so are the trade winds [*Brierley et al.*, 2009]. The land-sea contrast (critical for the West African monsoon) remains approximately constant with the reduction in the meridional SST gradient; however, the monsoon cannot penetrate as far north against the strengthened trade winds. The intensification of the Hadley circulation also leads to a stronger upper level tropical jet in the summer. This stronger jet suppresses high cloud formation in a broad swath along 30°N leading to reduction in the longwave cloud forcing of ~40 W m^{-2}.

[46] Zonal SST gradients also have strong impacts on the hydrological cycle, causing a widespread drying throughout the year (Figure 9, bottom). The main branch of the modern Walker circulation involves uplift over Indonesia and subsidence over the east Pacific. However, there is a minor branch over the Indian Ocean, with subsidence occurring over the coast of East Africa with associated colder SSTs. In the modern zonal simulation, the Walker circulation is extinguished (a consequence of prescribing zonally uniform SSTs). Thus, the drying of East Africa is caused by a suppression of penetrating convection by the subsidence related to the spin-up of the Walker cell.

[47] There are large changes in the moisture budget (precipitation minus evaporation, shown as line contours in Figure 9) over the Indian Ocean, especially in boreal summer. These are related to a dramatic strengthening of the summer monsoon, including the Somali jet. The strengthening of the summer monsoon brings a lot of moisture to India but makes East Africa drier (as the moisture from the Indian Ocean no longer heads toward Africa). The response

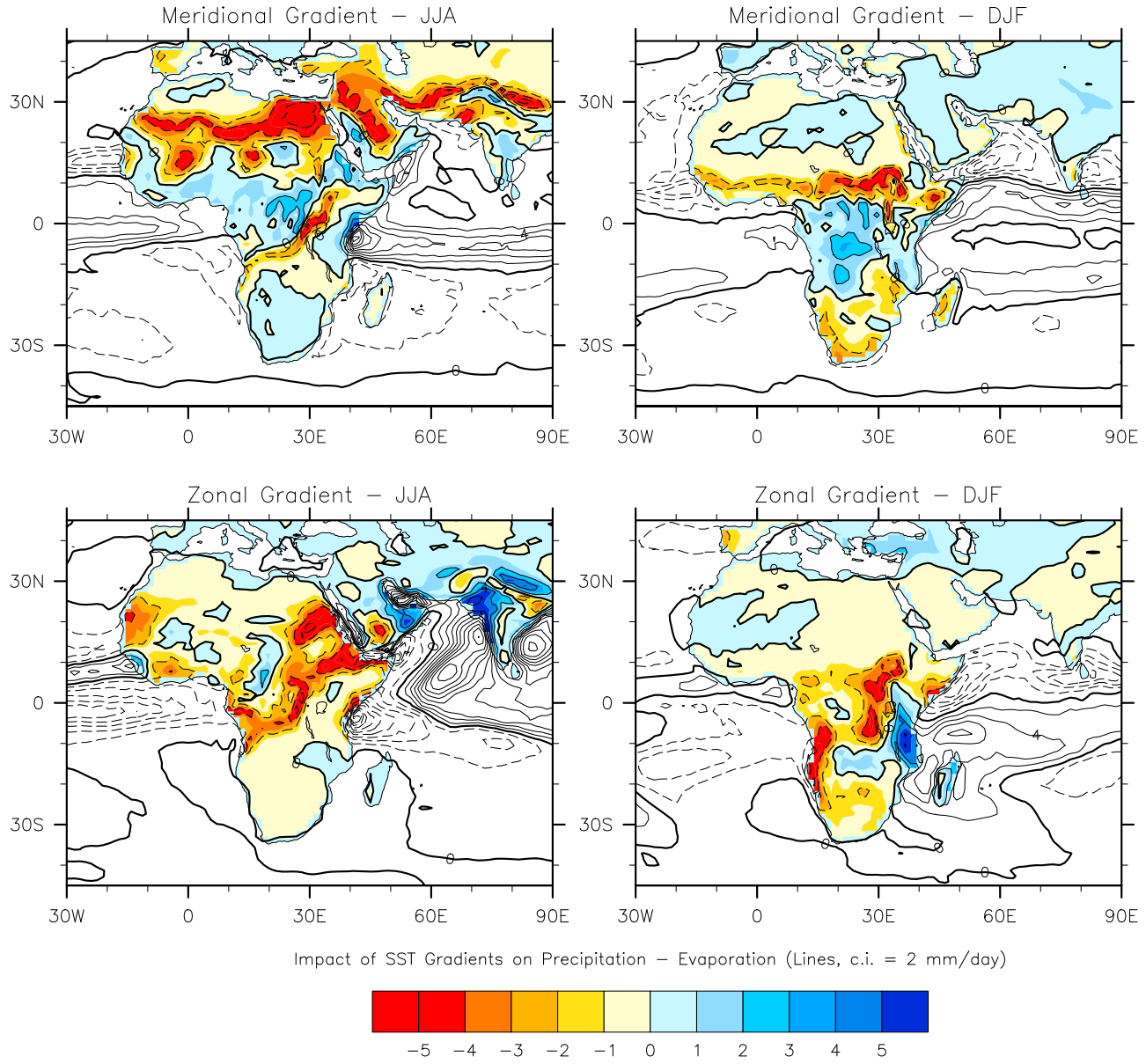

Figure 9. The impact of increasing meridional and zonal SST gradients on the P - E field over Africa and surrounding regions. (top) Impact of increasing the meridional SST gradient on (right) boreal summer and (left) boreal winter and (bottom) consequences of establishing modern zonal SST gradients on the same seasons. The colors show changes in P - E over land (in mm d^{-1}). The lines show changes in P - E with a contour interval of 2 mm d^{-1} over the ocean; the bold line corresponds to 0, and negative contours are dashed.

of the South Asian monsoon is stronger to changes in the zonal rather than meridional SST gradient in the tropics.

[48] Changes in monsoon characteristics before and during the Pliocene-Pleistocene interval have been a subject of a number of studies in the past, even though the exact timing and nature of these changes are still not entirely settled [*Huang et al.*, 2007; *Gupta and Thomas*, 2003]. Often the intensification of the South Asian monsoon is linked to the uplift of the Tibetan Plateau [*Clift and Plumb*, 2008; *Molnar et al.*, 2010; *Boos and Kuang*, 2010], but here, we show that the strengthening of the South Asian monsoon could be caused by SST changes alone rather than by orographic variations.

4. Discussion

[49] Clearly, there are a number of limitations affecting our study. First, with the way we define the meridional SST profile, we most likely underestimate changes in high-latitude SST, north of ~60°N. Taking into account the

cooling of the high-latitude ocean fully would further amplify the impacts of the reduction in the meridional SST gradient. The assumption of ocean basins that have zonally uniform SSTs (except for South Pacific) is also an idealization. The wind stress in all the simulations would drive ocean circulation, creating boundary currents and hence zonal temperature gradients (albeit rather weak according to observations [see *Fedorov et al.*, 2006; *Brierley et al.*, 2009; *Dekens et al.*, 2007]).

[50] Second, this work has not incorporated interactive ice sheets, so it is not possible to determine whether the impacts of the changes in SST gradients alone were sufficient to initiate glaciation. Overall, it is likely that SST changes worked in tandem with other environmental factors during the Pliocene, specifically with CO_2 variations. Likewise, our results are not sufficient to make definite conclusions about the impacts of meridional SST changes on the Greenland ice sheet. A more thorough analysis would be needed, perhaps similar to that by *Lunt et al.* [2008], who employed an offline ice sheet model and considered changes in CO_2, Greenland's tectonic uplift, and other factors but not the changes in the tropical meridional SST contrast.

[51] Our study is motivated in part by the results presented in Figure 1a: it is worth discussing the fidelity of these data (originating in the work of *Wara et al.* [2005] and *Brierley et al.* [2009]). The zonal temperature contrast is calculated as the difference between Mg/Ca proxy SST at Ocean Drilling Program (ODP) Site 806 in the western equatorial Pacific and ODP Site 847 in the eastern equatorial Pacific. These sites have been slowly converging because of plate tectonics [*Pisias et al.*, 1995]; however, this convergence can account for less than 0.5°C of the temperature changes seen over the past 4 Myr. Tectonics could have had a similarly small effect on the meridional SST gradient, which is calculated as the difference between alkenone SST (U_k^{37}-based) at ODP 846 in the east equatorial Pacific and ODP 1012 in the California margin. Although both sites have seen over 200 km of horizontal movement [*Pisias et al.*, 1995; *Lyle*, 1997], they have remained in the same oceanographic settings throughout the period. The locations of the four ODP sites at 4 Ma, 2 Ma, and the present-day are shown overlaid in Figures 3a, 3b, and 3c, respectively.

[52] There is a systematic difference between the temperature data from the two geochemical proxies mentioned above: alkenones can produce temperatures 0.5°C –1°C colder than the Mg/Ca proxy [*Dekens et al.*, 2008]. Because of this issue, and also because different ODP sites show somewhat different evolution of temperature in the eastern Pacific, the exact timing when the zonal SST gradient along the equator reached modern values differs from one study to the next [*Philander and Fedorov*, 2003; *Molnar and Cane*, 2002; *Wara et al.*, 2005; *Fedorov et al.*, 2006; *Lawrence et al.*, 2006].

[53] We have treated the SST changes over the past 4 Myr as two independent processes: an increase in the meridional gradient followed by an increase in the zonal gradient in the tropics. The justification of this treatment is the apparent different evolution of the two indices shown in Figure 1a and in the different responses of the atmospheric circulation to the two effects (for example, the two have opposite effects on the strength of the Hadley circulation). Furthermore, as argued by *Brierley et al.* [2009], the increase in the meridional SST gradient and the general cooling of the subtropics and midlatitudes are necessary conditions for the appearance of cold water in the equatorial upwelling region. Nevertheless, it is clear that in the full climate system, our treatment of the SST gradients as independent has certain limitations, for instance, because of nonlinearity of the atmospheric response.

[54] It has been suggested that potential aliasing in the proxy data can disguise changes in El Niño--Southern Oscillation (ENSO) frequency as a change in the zonal SST gradient along the equator: a characteristic of the mean state of the ocean [*Wunsch*, 2009]. Even though aliasing in the paleodata is a serious problem indeed, the abundance of data for the early Pliocene does indicate that the mean climate state then was very different from the present and cannot be simply explained by aliasing of the ENSO signal in paleorecords. For example, on ENSO timescales, the SSTs in the eastern equatorial Pacific are correlated to those in the California margin. However, variations in the latter temperatures do not exceed 1°C –2°C even for strong El Niño events. This is compared to a roughly 10°C temperature decrease in the California margin since the early Pliocene.

[55] Another important issue is the "low gradient paradox," that is, how to maintain a weak meridional temperature gradient (as in the early Pliocene) and a sufficiently strong poleward heat transport at the same time. Many studies emphasize this problem for hothouse climates such as the Eocene [e.g., *Huber and Sloan*, 1999]. *Brierley et al.* [2009] discuss this problem in relevance to the early Pliocene. The present study implicitly assumes that there exists a sufficient mechanism for transporting heat poleward but does not address the nature of this mechanism.

5. Conclusions

[56] Recently available SST estimates show that there have been significant changes in both meridional and zonal SST distribution over the past 4–5 Myr [*Fedorov et al.*, 2006; *Brierley et al.*, 2009]. Whereas the early Pliocene is characterized by weak meridional and zonal temperature gradients especially in the tropics and subtropics, subsequent climate evolution resulted in the development of more pronounced SST gradients. Eventually, a much stronger temperature contrast developed between the equator and the subtropics/midlatitudes and between the western and eastern parts of the equatorial Pacific. The latter occurrence signaled the demise of permanent El Niño-like conditions in the tropical region.

[57] Using simulations with an atmospheric general circulation model, we have investigated and compared various climatic impacts of the changes in meridional and zonal SST distributions. In particular, we have shown that both factors can facilitate the growth of ice sheets over North America. However, the impacts of the increasing meridional SST gradient are substantially larger that the impacts of changes in the zonal SST gradient. The timing of the development of the two gradients (Figure 1) provides additional clues, suggesting that the meridional gradient had started to

increase long before the zonal SST contrast reached modern values, even though the exact timing when the zonal SST gradient reached modern values differs between different proxies and different sites.

[58] The meridional SST gradients changes also appear to dominate global changes in average climate properties. For example, the shift to the modern meridional SST gradient in the model leads to a global mean temperature reduction of ~3.2°C versus ~0.6°C in case of the zonal changes. This is mainly due to a much greater reduction in the atmospheric water vapor content (which is a potent greenhouse gas) in the former case. These results indicate that reproducing the correct SST distribution appears to be critical for a model to account not only for the ice sheet inception and changes in precipitation but also to reproduce proper changes in the key elements of the global radiative forcing, such as the distribution of water vapor and cloud cover (both high and low clouds) in the atmosphere.

[59] Furthermore, the establishment of present-day meridional and zonal SST gradients leads to substantial regional-scale climate changes. The increase in meridional SST gradient causes a substantial aridification of the Sahara and the Arabian Peninsula, while the increase in zonal SST gradient causes similar drying elsewhere in Africa. The aridification of southwest Africa seen over the Pliocene-Pleistocene appears to be caused by changes in both zonal and meridional SST gradients.

[60] The South Asian monsoon is substantially strengthened, and its spatial distribution is altered with the establishment of zonal SST gradients. One of the consequences of this is the drying of East Africa. The monsoon strengthening in this study is caused by SST changes alone rather than by slow orographic variations as suggested by a number of authors [e.g., *Molnar et al.*, 2010; *Boos and Kuang*, 2010].

[61] Perhaps one of the most important questions that this study does not address is related to the ultimate causes of the changes in the SST gradients over the last 4–5 Myr or so. These causes are currently poorly understood; in general, they can be related to the reduction in the atmospheric CO_2 concentration since the early Pliocene [*Pagani et al.*, 2010], gradual shoaling of the ocean thermocline that culminated in the appearance of cold upwelling region in the ocean and led to ocean-atmosphere coupled feedbacks [*Philander and Fedorov*, 2003], or major changes in the atmospheric high-latitude circulation [*Gupta and Thomas*, 2003] or in the ocean circulation [*Bartoli et al.*, 2005]: all of these are amplified by climate feedbacks. Nevertheless, despite this uncertainty, from the results of this study, it appears very likely that the growth of Northern Hemisphere ice sheets was a result of the global, symmetrical with respect to the equator, cooling of Earth's climate since ~4 Ma rather than its initial cause.

[62] **Acknowledgments.** Financial support was provided by the grants to A.V.F. from the National Science Foundation (OCE-0550439 and OCE-0901921), Department of Energy Office of Science (DE-FG02-06ER64238, DE-FG02-08ER64590), and the David and Lucile Packard Foundation. This work was supported in part by the Yale University Faculty of Arts and Sciences High Performance Computing facility. We thank Brian Dobbins for help with computer simulations and Peter deMenocal, Gerald Dickens, and two anonymous reviewers for their help in improving the manuscript. A.V.F. thanks George Philander for numerous discussions of the topic.

References

Barreiro, M., G. Philander, R. Pacanowski, and A. Fedorov (2006), Simulations of warm tropical conditions with application to middle Pliocene atmospheres, *Clim. Dyn.*, *26*, 349–365, doi:10.1007/s00382-005-0086-4.

Barron, E. J. (1987), Eocene equator-to-pole surface ocean temperatures: A significant climate problem, *Paleoceanography*, *2*(6), 729–739, doi:10.1029/PA002i006p00729.

Bartoli, G., M. Sarnthein, M. Weinelt, H. Erlenkeuser, D. Garbe Schönberg, and D. W. Lea (2005), Final closure of Panama and the onset of Northern Hemisphere glaciation, *Earth Planet. Sci. Lett.*, *237*, 33–44, doi:10.1016/j.epsl.2005.06.020.

Bonham, S. G., A. M. Haywood, D. J. Lunt, M. Collins, and U. Salzmann (2009), El Nino-Southern Oscillation, Pliocene climate and equifinality, *Philos. Trans. R. Soc. A*, *367*, 127–156, doi:10.1098/rsta.2008.0212.

Boos, W. R., and Z. Kuang (2010), Dominant control of the South Asian monsoon by orographic insulation versus plateau heating, *Nature*, *463*, 218–222, doi:10.1038/nature08707.

Braithwaite, R. J., and Y. Zhang (2000), Sensitivity of mass balance of five Swiss glaciers to temperature changes assessed by tuning a degree-day model, *J. Glaciol.*, *46*(152), 7–14, doi:10.3189/172756500781833511.

Brayshaw, D. J., B. J. Hoskins, and M. Blackburn (2008), The storm-track response to idealized SST perturbations in an aquaplanet GCM, *J. Atmos. Sci.*, *65*(9), 2842–2860, doi:10.1175/2008JAS2657.1.

Brierley, C. M., A. V. Fedorov, Z. Lui, T. Herbert, K. Lawrence, and J. P. LaRiviere (2009), Greatly expanded tropical warm pool and weakened Hadley circulation in the early Pliocene, *Science*, *323*, 1714–1718, doi:10.1126/science.1167625.

Caballero, R., and P. L. Langen (2005), The dynamic range of poleward energy transport in an atmospheric general circulation model, *Geophys. Res. Lett.*, *32*, L02705, doi:10.1029/2004GL021581.

Clift, P. D., and R. Alan Plumb (2008), *The Asian Monsoon: Causes, History and Effects*, 288 pp., doi:10.1017/CBO9780511535833, Cambridge Univ. Press, Cambridge, U. K.

Collins, W. D., P. J. Rasch, B. A. Boville, J. J. Hack, J. R. McCaa, D. L. Williamson, B. P. Briegleb, C. M. Bitz, S.-J. Lin, and M. Zhang (2006), The formulation and atmospheric simulation of the Community Atmosphere Model: CAM3, *J. Clim.*, *19*(11), 2144–2161, doi:10.1175/JCLI3760.1.

Dekens, P. S., A. C. Ravelo, and M. D. McCarthy (2007), Warm upwelling regions in the Pliocene warm period, *Paleoceanography*, *22*, PA3211, doi:10.1029/2006PA001394.

Dekens, P. S., A. C. Ravelo, M. D. McCarthy, and C. A. Edwards (2008), A 5 million year comparison of Mg/Ca and alkenone paleothermometers, *Geochem. Geophys. Geosyst.*, *9*, Q10001, doi:10.1029/2007GC001931.

deMenocal, P. (2004), African climate change and faunal evolution during the Pliocene-Pleistocene, *Earth Planet. Sci. Lett.*, *220*(1–2), 3–24, doi:10.1016/S0012-821X(04)00003-2.

Deser, C., A. Capotondi, R. Saravanan, and A. Phillips (2006), Tropical Pacific and Atlantic climate variability in CCSM3, *J. Clim.*, *19*(11), 2451–2481, doi:10.1175/JCLI3759.1.

Dowsett, H. J., and M. M. Robinson (2009), Mid-Pliocene equatorial Pacific sea surface temperature reconstruction: A multi-proxy perspective, *Philos. Trans. R. Soc. A*, *367*, 109–125, doi:10.1098/rsta.2008.0206.

Dupont, L. M., B. Donner, L. Vidal, E. M. Perez, and G. Wefer (2005), Linking desert evolution and coastal upwelling: Pliocene climate change in Namibia, *Geology*, *33*(6), 461–464, doi:10.1130/G21401.1.

Emanuel, K. (1995), On thermally direct circulations in moist atmospheres, *J. Atmos. Sci.*, *52*(9), 1529–1536, doi:10.1175/1520-0469(1995)052<1529:OTDCIM>2.0.CO;2.

Fedorov, A. V., P. S. Dekens, M. McCarthy, A. C. Ravelo, P. B. deMenocal, M. Barreiro, R. C. Pacanowski, and S. G. Philander (2006), The Pliocene paradox (mechanisms for a permanent El Niño), *Science*, *312*, 1485–1489, doi:10.1126/science.1122666.

Fedorov, A. V., C. Brierley, and K. Emanuel (2010), Tropical cyclones and permanent El Niño in the early Pliocene, *Nature*, *463*, 1066–1070, doi:10.1038/nature08831.

Gibbard, P. L., M. J. Head, and M. J. C. Walker, and the Subcommission on Quaternary Stratigraphy (2009), Formal ratification of the Quaternary system/period and the Pleistocene series/epoch with a base at 2.58 Ma, *J. Quat. Sci.*, *25*, 96–102, doi:10.1002/jqs.1338.

Green, P. M., D. M. Legler, C. J. Miranda V, and J. J. O'Brien (1997), The North American climate patterns associated with the El Niño-Southern Oscillation, *COAPS Proj. Rep. Ser. 97–1*, Cent. for Ocean-Atmos. Predict. Stud., Fla. State Univ., Tallahassee.

Greuell, W., and C. Genthon (2004), Modelling land-ice surface mass balance, in *Mass Balance of the Cryosphere: Observations and Modelling of Contemporary and Future Changes*, edited by J. L. Bamber and A. J. Payne, pp. 117–168, Cambridge Univ. Press, Cambridge, U. K., doi:10.1017/CBO9780511535659.007.

Gupta, A., and E. Thomas (2003), Initiation of Northern Hemisphere glaciation and strengthening of the northeast Indian monsoon: Ocean Drilling Program Site 758, eastern equatorial Indian Ocean, *Geology*, *31*(1), 47–50, doi:10.1130/0091-7613(2003)031<0047:IONHGA>2.0.CO;2.

Haug, G., D. Sigman, R. Tiedemann, T. Pedersen, and M. Sarnthein (1999), Onset of permanent stratification in the subarctic Pacific Ocean, *Nature*, *401*(6755), 779–782, doi:10.1038/44550.

Haywood, A. M., and P. J. Valdes (2004), Modelling Pliocene warmth: Contribution of atmosphere, oceans and cryosphere, *Earth Planet. Sci. Lett.*, *218*, 363–377, doi:10.1016/S0012-821X(03)00685-X.

Haywood, A. M., P. J. Valdes, and V. L. Peck (2007), A permanent El Niño-like state during the Pliocene?, *Paleoceanography*, *22*, PA1213, doi:10.1029/2006PA001323.

Huang, Y., S. C. Clemens, W. Liu, Y. Wang, and W. L. Prell (2007), Large-scale hydrological change drove the late Miocene C-4 plant expansion in the Himalayan foreland and Arabian Peninsula, *Geology*, *35*(6), 531–534, doi:10.1130/G23666A.1.

Huber, M., and L. C. Sloan (1999), Warm climate transitions: A general circulation modeling study of the late Paleocene thermal maximum (about 56 Ma), *J. Geophys. Res.*, *104*(D14), 16,633–16,655, doi:10.1029/1999JD900272.

Huybers, P., and P. Molnar (2007), Tropical cooling and the onset of North American glaciation, *Clim. Past*, *3*(3), 549–557, doi:10.5194/cp-3-549-2007.

Laskar, J., P. Robutel, F. Joutel, M. Gastineau, A. C. M. Correia, and B. Levrard (2004), A long-term numerical solution for the insolation quantities of the Earth, *Astron. Astrophys.*, *428*, 261–285, doi:10.1051/0004-6361:20041335.

Lawrence, K. T., Z. Liu, and T. D. Herbert (2006), Evolution of the eastern tropical Pacific through Plio-Pleistocene glaciation, *Science*, *312*, 79–83, doi:10.1126/science.1120395.

Lindzen, R., and S. Nigam (1987), On the role of sea surface temperature gradients in forcing low-level winds and convergence in the tropics, *J. Atmos. Sci.*, *44*(17), 2418–2436, doi:10.1175/1520-0469(1987)044<2418:OTROSS>2.0.CO;2.

Lisiecki, L. E., and M. E. Raymo (2005), A Pliocene-Pleistocene stack of 57 globally distributed benthic $\delta^{18}O$ records, *Paleoceanography*, *20*, PA1003, doi:10.1029/2004PA001071.

Lunt, D. J., G. L. Foster, A. M. Haywood, and E. J. Stone (2008), Late Pliocene Greenland glaciation controlled by a decline in atmospheric CO_2 levels, *Nature*, *454*(7208), 1102–1105, doi:10.1038/nature07223.

Lyle, M. (1997), Reconstructed geographic positions and water depths for Leg 167 drill sites, *Proc. Ocean Drill. Program, Initial Rep.*, *167*, 41–46, doi:10.2973/odp.proc.ir.167.103.1997.

Marlow, J. R., C. B. Lange, G. Wefer, and A. Rosell-Mele (2000), Upwelling intensification as part of the Pliocene-Pleistocene climate transition, *Science*, *290*, 2288–2291, doi:10.1126/science.290.5500.2288.

Molnar, P., and M. A. Cane (2002), El Niño's tropical climate and teleconnections as a blueprint for pre-Ice Age climates, *Paleoceanography*, *17*(2), 1021, doi:10.1029/2001PA000663.

Molnar, P., W. R. Boos, and D. S. Battisti (2010), Orographic controls on climate and paleoclimate of Asia: Thermal and mechanical roles for the Tibetan Plateau, *Annu. Rev. Earth Planet. Sci.*, in press.

Muller, R. A., and G. J. MacDonald (2000), *Ice Ages and Astronomical Causes: Data, Spectral Analysis and Mechanisms*, 318 pp., Springer, Berlin.

Nathan, S., and R. M. Leckie (2009), Early history of the western Pacific warm pool during the middle to late Miocene (~13.2–5.8Ma): Role of sea-level change and implications for equatorial circulation, *Palaeogeogr. Palaeoclimatol. Palaeoecol.*, *274*, 140–159, doi:10.1016/j.palaeo.2009.01.007.

Neale, R. B., and B. J. Hoskins (2000), A standard test for AGCMs including their physical parametrizations: I: The proposal, *Atmos. Sci. Lett.*, *1*(2), 101–107, doi:10.1006/asle.2000.0019.

Pagani, M., Z. Lui, J. LaRiviere, and A. C. Ravelo (2010), High Earth-system climate sensitivity determined from Pliocene carbon dioxide concentrations, *Nat. Geosci.*, *3*, 27–30, doi:10.1038/ngeo724.

Philander, S. G., and A. V. Fedorov (2003), Role of tropics in changing the response to Milankovich forcing some three million years ago, *Paleoceanography*, *18*(2), 1045, doi:10.1029/2002PA000837.

Pisias, N., L. Mayer, and A. Mix (1995), Paleoceanography of the eastern equatorial Pacific during the Neogene: Synthesis of Leg 138 drilling results, *Proc. Ocean Drill. Program, Sci. Results*, *138*, 5–21, doi:10.2973/odp.proc.sr.138.101.1995.

Plumb, R.A., and A. Y. Hou (1992), The response of a zonally symmetric atmosphere to subtropical thermal forcing: Threshold behavior, *J. Atmos. Sci.*, *49*, 1790–1799, doi:10.1175/1520-0469(1992)049<1790:TROAZS>2.0.CO;2.

Ravelo, A. C., D. H. Andreasen, M. Lyle, A. O. Lyle, and M. W. Wara (2004), Regional climate shifts caused by gradual global cooling in the Pliocene epoch, *Nature*, *429*(6989), 263–267, doi:10.1038/nature02567.

Raymo, M. E., and P. Huybers (2008), Unlocking the mysteries of the ice ages, *Nature*, *451*(7176), 284–285, doi:10.1038/nature06589.

Rayner, N. A., D. E. Parker, E. B. Horton, C. K. Folland, L. V. Alexander, D. P. Rowell, E. C. Kent, and A. Kaplan (2003), Global analyses of sea surface temperature, sea ice, and night marine air temperature since the late nineteenth century, *J. Geophys. Res.*, *108*(D14), 4407, doi:10.1029/2002JD002670.

Sepulchre, P., G. Ramstein, F. Fluteau, M. Schuster, J. J. Tiercelin, and M. Brunet (2006), Tectonic uplift and eastern Africa aridification, *Science*, *313*, 1419, doi:10.1126/science.1129158.

Wara, M. W., A. C. Ravelo, and M. L. Delaney (2005), Permanent El Niño-like conditions during the Pliocene warm period, *Science*, *309*, 758–761, doi:10.1126/science.1112596.

Wunsch, C. (2009), A perpetually running ENSO in the Pliocene? *J. Clim.*, *22*, 3506–3510, doi:10.1175/2009JCLI2925.1.

Zachos, J., M. Pagani, L. Sloan, E. Thomas, and K. Billups (2001), Trends, rhythms, and aberrations in global climate 65 Ma to present, *Science*, *292*, 686–693, doi:10.1126/science.1059412.

C. M. Brierley and A. V. Fedorov, Department of Geology and Geophysics, Yale University, 210 Whitney Ave., New Haven, CT 06511, USA. (christopher.brierley@yale.edu; alexey.fedorov@yale.edu)